

Adaptive Variable Structure Interacting Multiple Model Tracking Algorithm for Hypersonic Glide Vehicle

Zhumu Fu^{1,2} , Dongfeng Wan¹ , Zhikai Wang^{1,*} , Fazhan Tao¹ 

1. Henan University of Science and Technology  – School Information Engineering – Luoyang Henan – China.

2. National Key Laboratory of Air-based Information Perception and Fusion  – Luoyang Henan – China.

*Correspondence author: zhikaiwang01@163.com

ABSTRACT

During the penetration process of hypersonic glide vehicles (HGV), the maneuvering forms are varied, which brings some challenges for tracking them, such as difficulty in the stable matching of single-model tracking and the slow response of multi-model tracking. Therefore, this paper proposes an improved adaptive variable structure interacting multiple model tracking algorithm by analyzing the maneuvering characteristics of the target. The algorithm can switch between interacting multiple models and single-model tracking by defining a set of model-switching conditions. Additionally, it designs two correction functions and embeds them into the model probability update phase of the adaptive variable structure interacting multiple model algorithm, so that the proposed adaptive variable structure interacting multiple model algorithm can adaptively adjust the transition probability matrix (TPM) according to the probability law of the target maneuver model. Finally, the effectiveness and superiority of the proposed algorithm were verified through comparative simulation experiments with existing algorithms. Compared with the single-model tracking algorithm, the proposed algorithm's position root mean square error is significantly reduced by nearly one-third, while also reducing the single running time by nearly one-fourth compared to other multi-model tracking algorithms.

Keywords: Hypersonic gliders; Mathematical models; Radar tracking; Adaptive control.

INTRODUCTION

Due to the characteristics of high speed and complex aerodynamic structure, hypersonic glide vehicles (HGV) can perform complex maneuvering strategies, such as wave maneuvers, jump maneuvers, and spiral maneuvers, resulting in complex and unpredictable trajectories, which brings challenges to the continuous estimation and tracking of HGV (Yu and Chen 2021; Song *et al.* 2021). In addition, the flight path design of HGV exhibits significant degrees of freedom. Capable of executing various evasion and penetration maneuvers within known defense areas, HGV can even employ extensive lateral maneuvers to change the intended target of attack (Xu *et al.* 2022). This capability enables them to effectively evade interception by existing air defense systems, facilitating long-range and high-precision strikes. This attack mode has become an effective means of attack in modern wars. Predicting the trajectory of HGV is one of the important methods to improve the interception probability of air defense systems, and accurate tracking of HGV is a prerequisite for trajectory prediction.

Effective target tracking entails extracting valuable information regarding the target's motion state from noisy observations. This outcome heavily relies on the employed target motion model and filtering algorithm, particularly when the error statistics of the sensor under evaluation are known. To describe common target motion, the kinematic characteristics of the target are used

Received: Jul. 17, 2024 | **Accepted:** Oct. 09, 2024

Section editor: Luiz Martins-Filho 

Peer Review History: Single Blind Peer Review



to model the unknown maneuver, such as the Singer model (Jia *et al.* 2017), the current statistical model (Sun and Yang 2016), and the Jerk model (Feng *et al.* 2020). Drawing from an analysis of the trajectory attributes specific to the periodic ski-jump type, a sine model was introduced in Wang *et al.* (2015). This model represents the target acceleration as a sine wave autocorrelation random process, facilitating the tracking of ski-jump moving targets. A damped oscillation model is proposed in Li *et al.* (2020), and a parameter adaptive method based on jump point identification is designed to track near-space HGV. Simulation experiments are conducted to validate the feasibility and effectiveness of both the damped oscillation model and the adaptive method. Based on the damped oscillation model, an adaptive non-zero mean damped oscillation model based on the mean compensation idea is proposed in Li *et al.* (2022) for tracking near-space HGV. Comparative analysis against the sine model and damped oscillation model reveals that the adaptive non-zero mean damped oscillation model offers distinct advantages in terms of tracking accuracy and operational efficiency. In Cheng *et al.* (2021), presents an adaptive non-zero mean damped oscillation model was presented, founded on the HGV maneuver mode. Comparative analysis against the traditional sine model and Singer model demonstrates that the adaptive non-zero mean damped oscillation model offers enhanced tracking accuracy and exhibits reasonable convergence. Nevertheless, in many scenarios, it remains challenging for a singular fixed model to cover the whole process of maneuvering targets.

The ongoing advancement in control and guidance technology has led to increased flexibility in the maneuvering capabilities of HGV. To better align the motion model with the actual trajectory of HGV, the emergence of multi-model algorithms has become imperative. The IMM algorithm utilizes multiple mathematical models to approximate the actual movement of the target, with each model operating in parallel. Model probabilities are adjusted using Markov coefficients to enhance tracking performance (Luo Y *et al.* 2022). Because the motion of a single model cannot accurately describe the motion state of the target relative to the radar, in order to improve the accuracy of the description of the target motion state, Jiang and Zhou. (2022) proposed the interactive multiple model strong tracking unscented Kalman filter (IMM-STUKF) algorithm, which solved the problem of inaccurate description of the actual motion state of the target. An adaptive IMM algorithm based on fuzzy control was introduced in Zhao *et al.* (2021). This algorithm employs a nonlinear mapping approach to process model probabilities in real-time, thereby screening model subsets, eliminating redundant models, enhancing the significance of valuable models, and automatically adjusting process noise levels through fuzzy inference mechanisms. Such enhancements render the algorithm more adaptable to various target maneuvering patterns. However, the aforementioned algorithms consider the transition probability matrix (TPM) as a constant matrix, which cannot adaptively describe the dynamic changes in the target's maneuver mode.

In the traditional IMM algorithm, the practice of setting TPM to a fixed value poses certain limitations. This is because an inappropriate TPM or system fluctuations can result in inaccurate state estimation. To enhance the efficacy of the IMM algorithm, the TPM can be adaptively updated based on current system model information. For example, a transition probability correction function that integrates past model information and selectively employs parallel IMM algorithms based on likelihood ratios was proposed in Xie *et al.* (2019). Their methodology effectively addresses issues like response lag and peak estimation errors by introducing a submodel jump threshold. However, in scenarios with numerous subfilter models, the algorithm management may become challenging due to the complexity of the parallel approach, potentially impacting robustness as it relies on a submodel jump threshold. Biao *et al.* (2021) put forward the model probability of updating the target by using the current measurement information and uses the updated model probability for hybrid prediction, thus improving the filtering performance of the algorithm to a certain extent. In order to adaptively calculate the TPM of the models in Li *et al.* (2021), by using the intersection degree between fuzzy sets, the probability switching model based on semantic fuzzy sets is derived, and the switching between semantic fuzzy sets is realized. In addition, Ye *et al.* (2020) introduced a novel correction factor and leveraged posterior information to dynamically adjust the TPM, enhancing the probability of model matching and improving tracking accuracy. In multi-model tracking, the computational time tends to increase exponentially with the growing number of models, leading to computational redundancy. Therefore, how to reduce the computational complexity of the IMM algorithm is one of the key issues addressed in this paper.

Besides, in the IMM based target tracking framework, the nonlinear filter is an important part of it. The extended Kalman filter (Montañez *et al.* 2023) has been extensively employed within interactive multi-model frameworks. Its fundamental principle involves locally linearizing nonlinear equations via Taylor series expansion, followed by signal filtering based on Kalman filtering principles (Jordi and Damien 2020) (Wang *et al.* 2020). In situations where the degree of nonlinearity is minimal, the extended Kalman filter typically exhibits superior filtering performance. However, the extended Kalman filter necessitates the computation of the Jacobian

matrix for nonlinear functions, which in complex model systems can introduce computational complexity and the potential for errors, consequently diminishing filtering efficacy. Therefore, to enhance filtering accuracy and efficiency to address the demands of specific problems, researchers have investigated novel approximation methods, such as the unscented Kalman filter (Garcia-Fernandez *et al.* 2012) and particle filter (Li *et al.* 2016). In view of the tracking target of this paper being a hypersonic maneuvering target, which is a highly nonlinear system, compared with the extended Kalman filter, the unscented Kalman filter does not require approximating nonlinear functions, thus avoiding errors resulting from linearization and achieving higher filtering accuracy. Besides, unlike the particle filter, which approximates the probability distribution of the state using a large number of particles (samples), the unscented Kalman filter approximates the state distribution through specific Sigma points, resulting in better computational efficiency.

In a real combat environment, changes in the maneuvering mode of the target take a relatively small amount of time. In general, targets prefer to use a single maneuver mode, such as constant velocity (CV), constant acceleration (CA), or serpentine maneuvers. Therefore, when employing the IMM algorithm for target tracking, typically only one of the models dominates, leading to computational redundancy. To address this issue, an adaptive variable structure IMM algorithm is proposed in this paper. The fundamental concept of this algorithm is to dynamically switch between single and multi-model approaches based on the target's movement mode. Additionally, it incorporates two correction functions designed for adaptively updating the TPM within the interactive multi-model framework. This integration aims to enhance tracking precision while minimizing computational redundancy.

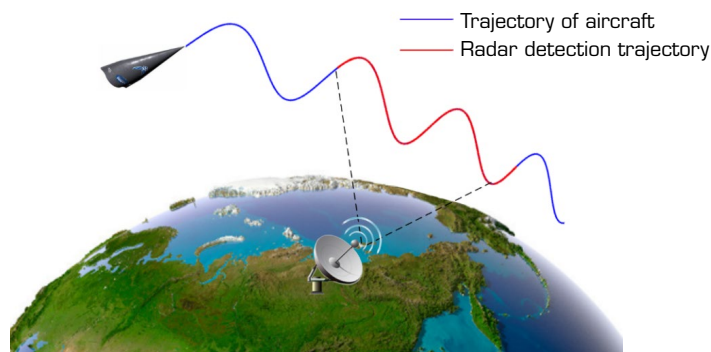
The main contributions of this paper are as follows:

- In this paper, two functions are designed to dynamically adjust the Markov TPM. These functions are integrated into the model probability update of the IMM tracking algorithm. This integration enhances the system's resistance to noise and addresses the issue of slow response during model transitions in multi-model tracking algorithms.
- By designing a switch strategy with two predefined thresholds, the system dynamically selects between the single-model or multi-model tracking algorithms. This strategy avoids the difficulty of stable matching difficulty in single-model tracking and mitigates the computational redundancy associated with multi-model tracking algorithms.

The subsequent sections of this paper are structured as follows: the next section briefly describes the kinematic tracking model and measurement equations of the HGV. The specific implementation process of the proposed adaptive variable structure IMM algorithm is provided in the Methodology section. The Simulation section shows the simulation results and performance comparison for the maneuvering tracking problems. Finally, the conclusions of this paper are summarized in the Conclusion section.

Radar-target relative motion modeling

The near-space HGV, outfitted with a composite control of the response control system and aerodynamic rudder, leverages its distinctive aerodynamic configuration to generate lift. It executes pull-up maneuvers to regulate flight altitude and speed, facilitating periodic ski-jump maneuvers. Consequently, the glide phase is more susceptible to interception (Zhang *et al.* 2022). This paper focuses on analyzing and tracking the trajectory of the unpowered glide phase, with the objective of refining the accuracy of fire control data for mid-course guidance of defense missiles. Furthermore, it provides a radar detection and tracking diagram, as depicted in the following in Fig. 1.



Source: Elaborated by the authors.

Figure 1. Schematic diagram of radar detection and tracking of hypersonic vehicle.

Hypersonic glide vehicles trajectory model

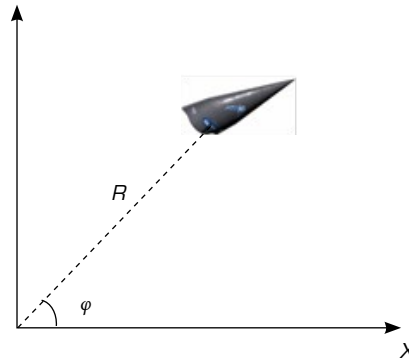
To accurately portray the movement of a hypersonic maneuvering target in near space, establishing a dynamic model is essential. Assuming Earth as a rotating positive sphere with CV, the dynamics model for an HGV can be formulated (Yu *et al.* 2019):

$$\begin{cases} \dot{r} = v \sin \gamma \\ \dot{\theta} = \frac{v \cos \gamma \cos \psi}{r \cos \phi} \\ \dot{\phi} = \frac{v \cos \gamma \sin \psi}{r} \\ \dot{v} = -\frac{D}{m} - g \sin \gamma + \omega^2 r \cos \phi (\cos \phi \sin \gamma - \sin \phi \cos \gamma \sin \psi) \\ \dot{\gamma} = \frac{L \cos \sigma}{mv} + \frac{v}{r} \cos \gamma - \frac{g}{v} \cos \gamma + 2\omega \cos \phi \cos \psi \\ \quad + \frac{\omega^2 r}{v} \cos \phi (\cos \phi \cos \gamma + \sin \phi \sin \gamma \sin \psi) \\ \dot{\psi} = -\frac{L^2 \sin \sigma}{mv \cos \gamma} - \frac{v}{r} \tan \phi \cos \gamma \cos \psi + 2\omega (\cos \phi \tan \gamma \sin \psi - \sin \phi) \\ \quad - \frac{\omega^2 r}{v \cos \gamma} \cos \phi \sin \phi \cos \psi \end{cases} \quad (1)$$

where r is the distance from the target to the Earth's center of mass O_e , θ and ϕ denote the longitude and latitude, respectively, v is the target speed, γ and ψ are the trajectory inclination and deflection angle, respectively, L and D represent the lift and drag forces, respectively, $g = 9.81 \text{ m/s}^2$ is the gravitational acceleration, m stands for the mass of the aircraft, ω typifies the Earth's rotation rate, and σ is the velocity inclination angle.

Radar measurement equation

In radar tracking systems, measurement data is typically presented in a polar coordinate system. The information provided by ground-based radar includes relative distance R and azimuth angle ϕ . The radar measurement information is illustrated in Fig. 2.



Source: Elaborated by the authors.

Figure 2. Information map of radar measurement.

The sensor measurement equation can be expressed as:

$$Z(k) = HX(k) + V(k) \quad (2)$$

where $Z(k) = [R, \phi]^T$ represents the direction-finding quantity, H is the measurement matrix, $V(k)$ denotes Gaussian white noise with a zero mean, and its corresponding noise covariance matrix is $V(k)$.

METHODOLOGY

Aiming at the problem of low tracking accuracy in single-model algorithms and low computational efficiency of multi-model algorithms, this paper proposes an adaptive variable structure IMM tracking algorithm. This algorithm tries to make full use of various maneuvering modes of the HGV to adaptively track the target with high precision. In this algorithm, the tracking process is categorized into the following three cases:

When the maximum value of model probability in the model set exceeds the threshold χ , single-model tracking is employed.

When the maximum value of model probability in the model set is below the threshold χ , multi-model tracking is used, but the maximum probability model remains unchanged during the use of multi-model tracking.

When the maximum value of model probability in the model set drops below the lower threshold χ , multi-model tracking is employed, but the maximum probability model changes during the use of multi-model tracking.

At the initial moment, since the probability of each model is one-third, which is less than the threshold χ , the IMM algorithm will be used. When $k > 1$, if the probability of model j is maximized, the maximum probability value is greater than the threshold χ , and the root mean square error ($RMSE$) ($k-1$) of the model j is less than the threshold ψ , the model j is used to track and calculate the $RMSE$; if the $RMSE(k)$ of model j exceeds the threshold ψ , indicating suboptimal tracking performance, the target is re-tracked using the IMM algorithm at time k ; if the probability of model j is maximized, but the maximum probability value is less than the threshold χ or the $RMSE(k-1)$ of the model j is greater than the threshold ψ , the IMM algorithm is directly used to track. The pseudocode of the proposed adaptive variable structure IMM algorithm is shown (Algorithm 1).

Algorithm 1. Proposed adaptive variable structure IMM algorithm.

```

Input : True value  $X_r$ , Measured value  $Z$ 
Output : Estimated value  $X_e$ ,  $RMSE$ 
Initialization: state variable value  $X(0)$ , TPM  $P(0)$ , Model probability  $\mu(0)$ 
begin
  for  $k = 1 : n$  do
    if max Probability > threshold  $\chi$ 
      if max Model Index == CV &  $RMSE_{CV}(k-1) < \text{threshold } \psi$ 
        ▶ :CV model track
        Calculate  $RMSE1$ 
        if  $RMSE1 > \text{threshold } \psi$ 
          ▶ :IMM track
        Calculate  $RMSE$ 
        continue
        else
          continue
      end
    else if max Model Index == CA &  $RMSE_{CA}(k-1) < \text{threshold } \psi$ 
      ▶ :CA model track
      Calculate  $RMSE2$ 
      if  $RMSE2 > \text{threshold } \psi$ 
        ▶ :IMM track
  end
  Continue...

```

Algorithm 1. Continuation.

```

    Calculate  $RMSE$ 
    continue
    else
    continue
  end
end
else if max Model Index == Sine &  $RMSE_{Sine}(k-1) < \text{threshold } \psi$ 
  ▶ :sine model track
  Calculate  $RMSE3$ 
  if  $RMSE3 > \text{threshold } \psi$ 
    ▶ :IMM track
    Calculate  $RMSE$ 
    continue
    else
    continue
    end
    else
    ▶ :IMM track
    Calculate  $RMSE$ 
  end
else
  ▶ :IMM track
  Calculate  $RMSE$ 
end
end

```

Single/multiple model adaptive switching

In this paper, three maneuvers commonly observed in the mid-course flight of hypersonic vehicles are chosen: CV, CA, and sine. Let μ_1 represent the probability of the CV model, μ_2 denote the probability of the CA model, and μ_3 signify the probability of the sine model, satisfying the following conditions:

$$\mu_1 + \mu_2 + \mu_3 = 1 \quad (3)$$

Considering the unknown initial motion mode of the HGV, employing an IMM algorithm is essential to track the target trajectory at the initial time (Guo and Teng 2022). Subsequently, the probability of a match model within the IMM framework is maximized. Once the probability of a specific model stabilizes and surpasses a predetermined threshold χ , the proposed algorithm transitions the tracking model from multiple models to a singular model. This transition is aimed at mitigating the computational redundancy inherent in the tracking algorithm. However, it is not possible for the target to maintain a constant motion pattern, and maneuvering is possible in subsequent tracking. When employing a single model for tracking, it becomes essential to assess whether the target tracking accuracy meets the desired criteria by utilizing the RMSE. If the RMSE value of target tracking exceeds a predefined threshold ψ , it indicates suboptimal performance in the single-model tracking. Consequently, there arises a necessity to transition from a single model to multiple models for re-tracking the maneuvering target at the current time. This measure ensures the accuracy of the tracking algorithm. Since multi-model tracking systems need to efficiently select and manage multiple models and switch between different models, the computational complexity and resource consumption increase significantly. In addition, in practice, the target motion pattern may change significantly. In this case, single-model tracking may not be able to effectively capture the dynamic changes of the target, resulting in increased

calculation errors and decreased tracking accuracy. The methodology proposed in this paper involves a dynamic switching mechanism between single and multiple models, effectively mitigating the computational complexity associated with utilizing multi-model tracking throughout the entire process.

Interacting multiple model algorithm based on adaptively updating TPM

The maximum probability model does not jump

In the multi-model object tracking algorithm, the estimated state of the system model is obtained by weighted summation of the likelihood functions of each model. The estimated state computed under the low-probability model may introduce noise into the overall estimated state. Therefore, increasing the probability value of the maximum probability model helps to improve the tracking accuracy of the IMM algorithm (Xie *et al.* 2019). Model jumps are guided by the TPM in the model interaction step. Therefore, the noise can be suppressed by properly defining the transition probability correction function to increase the probability value of the maximum probability model. Moreover, when the maximum probability model does not jump, the main error is caused by the noise of the current system model. If the TPM is modified by using the information of the model at the last moment, which is less affected by noise, the transition probability π_{ij} of the maximum probability model can be increased and the transition probability π_{ji} of the other models can be reduced. Based on the above analysis, a transition probability correction function is proposed. This function makes use of historical model information that is less susceptible to noise, thus minimizing its influence and facilitating the online learning of transition probabilities.

$$f(k) = \frac{1}{1-\beta} \quad (4)$$

In Eq. 4, β varying values are assigned to delineate the impact of past data on the current model probability. By substituting $\beta = \mu_j(k) - \mu_j(k-1)$ into Eq. 4, the transition probability correction function can be formally defined as follows:

$$f_j(k) = \frac{1}{1 - (\mu_j(k) - \mu_j(k-1))}, j = 1, 2, \dots, N \quad (5)$$

$$\hat{\pi}_{ij}(k) = f_j(k) * \pi_{ij}(k-1), (i = 1, 2, \dots, N) \quad (6)$$

By updating the TPM using Eq. 6, the anti-noise properties can also be achieved.

The maximum probability model jumping

In multi-model target tracking algorithms, when the matching model transitions from model i to model j , a slower transition time corresponds to a larger error (Lee and Park 2023). To minimize the transition time, an additional correction function is required for optimization purposes. Therefore, unlike Eq. 5, it must be sensitive to transformations of the model. When transitioning from model i to model j , the cross-difference model probability Δ can be utilized to examine the switching between models.

$$\Delta_j = \mu_j(k) - \sum_{i=1, i \neq j}^N \mu_i(k-1) \quad (7)$$

By defining the cross-difference model probability as the independent variable of Eq. 8, the calibration function is formulated as follows:

$$h_{ij}(k) = \frac{1}{1 + e^{-(\mu_j(k) - \sum_{i=1, i \neq j}^N \mu_i(k-1))}}, (j = 1, 2, \dots, N) \quad (8)$$

$$\hat{\pi}_{ij}(k) = h_{ij}(k) * \pi_{ij}(k-1), (i = 1, 2, \dots, N) \quad (9)$$



Algorithm 2. Proposed adaptive IMM algorithm.

Input : $z(k), \phi, \Gamma, H, \hat{X}_i(k-1/k-1), P_i(k-1/k-1)$

Output : $\hat{X}_i(k), P(k)$

Initialization: $X_0, P_0, Q_0, R_0, \mu_0, \pi_{ij}(0)$

for $k = 1 : \infty$ do

for $i = 1 : N$ do

► N : the number of modes

Model interaction:

for $j = 1 : N$ do

Predict μ_{k-1}^{ij}

end for

Calculate \hat{x}_{k-1}^{0i}

Calculate P_{k-1}^{0i}

2)Sub-Kalman filter model filtering:

Calculate x_k^i and P_k^i

3)Model probability calculation:

Calculate V_k^i

Calculate S_k^i

Calculate Λ_k^i

Calculate μ_k^i

for $j = 1 : N$ do

Calculate $f_j(k)$ using (5)

Calculate $\hat{\pi}_{ij}(k)$ using (6)

Calculate $h_{ij}(k)$ using (8)

Calculate $\hat{\pi}_{ij}(k)$ using (9)

Update $\pi_{ij}(k)$ using (10) and (11)

end for

end for

4)Estimate combination:

Calculate \hat{x}_k

Calculate P_k

end for

Equations 6 and 9 are integrated to represent the TPM. Therefore, we propose the integrated update TPM scheme as follows:

$$\hat{\pi}_{ij}(k) = (f_{ij}(k) - h_{ij}(k)) * \pi_{ij}(k-1) \quad (10)$$

Finally, normalization is performed to preserve the characteristics of the Markov process.

$$\pi_{ij}(k) = \frac{\hat{\pi}_{ij}(k)}{\sum_{j=1}^N \hat{\pi}_{ij}(k)} \quad (11)$$

Assume that the TPM is:

$$\Pi = \begin{bmatrix} \pi_{11} & \pi_{12} & \cdots & \pi_{1j} & \cdots & \pi_{1r} \\ \pi_{21} & \pi_{22} & \cdots & \pi_{2j} & \cdots & \pi_{2r} \\ \vdots & \vdots & \ddots & \vdots & \cdots & \vdots \\ \pi_{i1} & \pi_{i2} & \cdots & \pi_{ij} & \cdots & \pi_{ir} \\ \vdots & \vdots & \cdots & \vdots & \ddots & \vdots \\ \pi_{r1} & \pi_{r2} & \cdots & \pi_{rj} & \cdots & \pi_{rr} \end{bmatrix}$$

The variable r represents the number of models, while π_{ij} denotes the probability of transitioning from model i at time $k-1$ to model j at time k , $1 \leq i \leq r$, $1 \leq j \leq r$; obviously, for all models there are:

$$\sum_{j=1}^r \pi_{ij} = 1$$

The proposed algorithm sets two correction functions by using the current and previous model probability information to automatically update the TPM according to the situation and integrate it into the IMM algorithm.

Simulation

Parameter setting

In this section, by constructing a dataset and comparing the sine model algorithm, the classical IMM algorithm, the IMM algorithm based on quasi-Bayesian (IMM-QB) estimation (Jilkov and Li 2004), and the online probability transition matrix update with the proposed algorithm, it is verified that the proposed algorithm not only improves tracking accuracy, but also reduces the computational complexity. In this study, the computer configuration used includes the Lenovo Xiaoxin Pro 16 (2023), featuring an AMD Ryzen 7 7535HS processor with six cores and 12 threads. It is equipped with 16 GB of DDR5 RAM and a 512 GB NVMe SSD for fast storage and data access. The simulation parameters are outlined in Tables 1 and 2.

In this part, four different target trajectories are generated to verify the effectiveness of the proposed algorithm. The initial altitude, velocity, and the radar position of the four trajectories are all the same; the different trajectories are generated by modifying the maneuver acceleration of the aircraft. The red curve denotes the trajectories detected by radar.

The velocity curves of the HGV are shown in Fig. 4a, where the maneuver of the target occurs mainly in the y -direction during the gliding segment. The flight mode has the characteristics of strong maneuvering penetration capability, long range, and low energy consumption. Furthermore, Fig. 4b indicates that the acceleration of the HGV trajectory in the y -direction oscillates within a certain range. As flight time progresses, the flight speed gradually diminishes, accompanied by a reduction in the jump amplitude. Consequently, this paper focuses solely on tracking the target in the X - Y two-dimensional plane to validate the effectiveness of the proposed algorithm.



Table 1. Initial state of HGV in simulation

Initial states	Symbol	Value
Ordinate	Y	70,000m
Abscissa	X	0 m
Velocity	V	19.5 Ma
Mass	m	1,507 kg
Surface area	S	0.4839 m ²
Aerodynamic drag coefficient	C_D	0.157
Aerodynamic lift coefficient	C_L	0.490

Source: Elaborated by the authors.

Table 2. Parameter setting of radar and environment

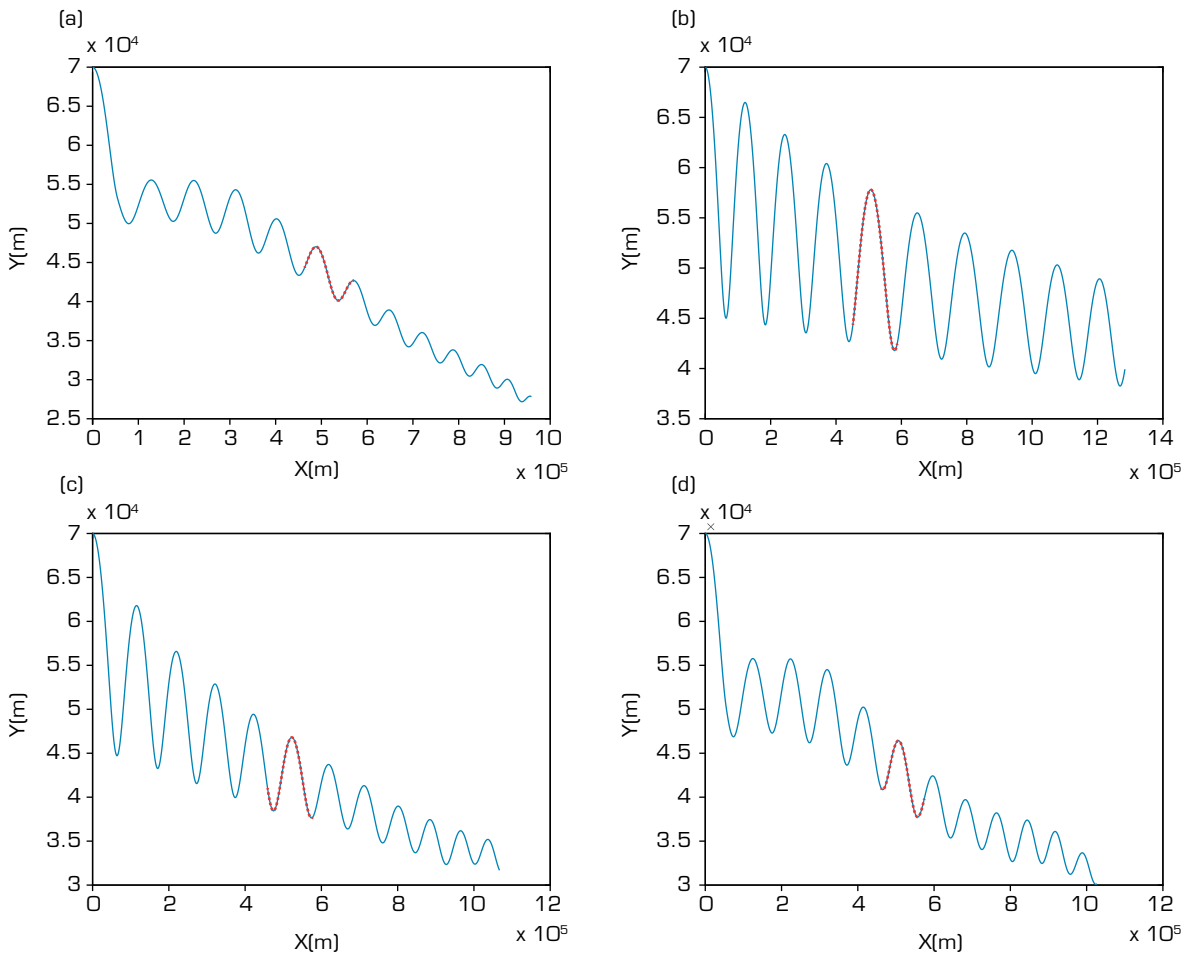
Parameter type	Parameter	Value
Radar parameter	Sampling rate	0.1 s
	Geographic coordinates	$[5.1713 \times 10^6 \text{ m } 0 \text{ m}]$
	Distance error	500 m
	Azimuth angle error	0.1°
Environmental parameter	Atmospheric density constant	1.22kg/m ³
	Earth gravitational constant	$3.99 \times 10^{14} \text{ m}^3/\text{s}^2$
	Earth rotation rate	$7.29 \times 10^{-5} \text{ rad/s}$
	Earth radius	6,378 km

Source: Elaborated by the authors.

Given that the radar detection azimuth has a measurement range of $A_r \in [-90^\circ, 90^\circ]$ and a detection range of 550 km, the paper solely tracks the segment of the target's trajectory detected by the radar during its flight. The observable segment of the trajectory in the inertial coordinate system of the target radar is illustrated in Fig. 3.

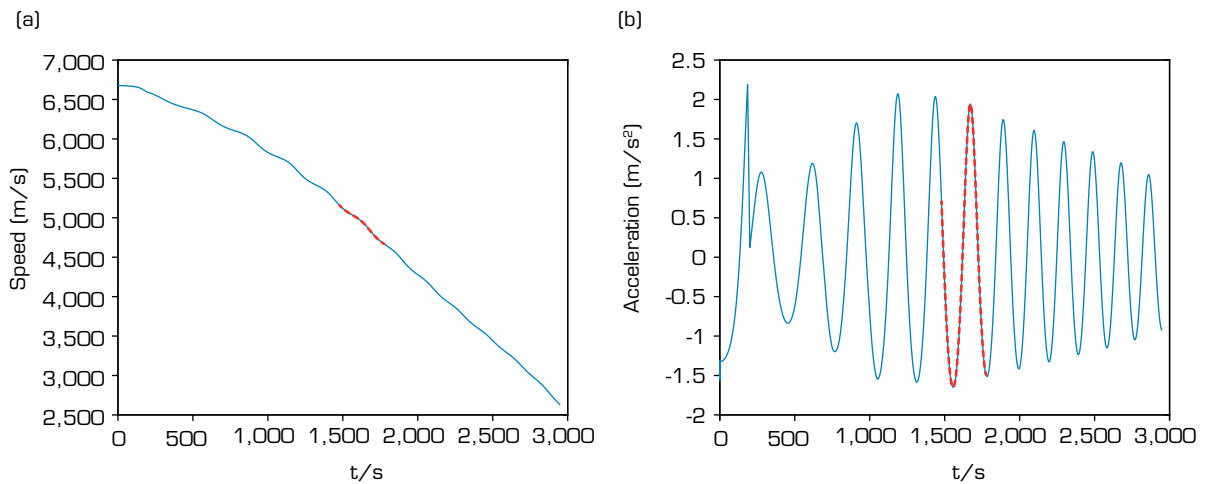
The target's state vector encompasses position, velocity, and acceleration in the X and Y directions. When generating a standard trajectory within the radar detection range, the state vector is structured as follows: $X(k) = [x, y, \dot{x}, \dot{y}, \ddot{x}, \ddot{y}]$, the simulation initial values for trajectory 1 of the target in the simulation can be expressed as follows: $X(0) = [4633400; 44345; 3595.3; 50.0375; 0.1362; 0.7066]$; the simulation initial values for trajectory 2 of the target in the simulation can be expressed as follows: $X(0) = [4514895; 44345; 4294.6; 112; 1.43; 2.975]$; the simulation initial values for trajectory 3 of the target in the simulation can be expressed as follows: $X(0) = [4588469; 41027; 3887.6; -114; 0.922; 1.476]$; and the simulation initial values for trajectory 4 of the target in the simulation can be expressed as follows: $X(0) = [4611919; 41030; 3749.1; -31.7; 0.115; 2.792]$. The probability of each model is one-third at the initial time. The TPM at the initial time is as follows:

$$P = \begin{bmatrix} 0.9 & 0.05 & 0.05 \\ 0.05 & 0.9 & 0.05 \\ 0.05 & 0.05 & 0.9 \end{bmatrix}$$



Source: Elaborated by the authors.

Figure 3. Trajectories of four different target maneuvers. (a) Trajectory 1 of the target; (b) Trajectory 2 of the target; (c) Trajectory 3 of the target; (d) Trajectory 4 of the target.



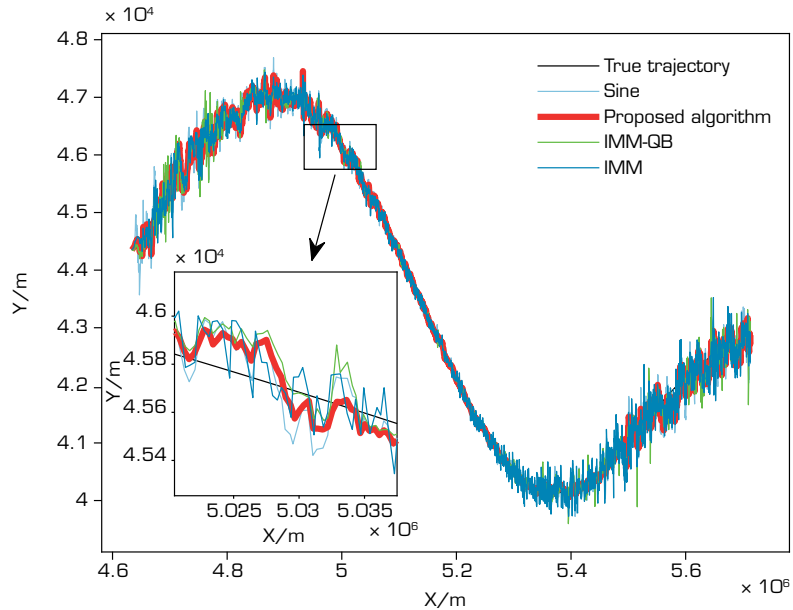
Source: Elaborated by the authors.

Figure 4. The target trajectory 1 speed and acceleration over time. (a) Speed; (b) Acceleration in the y-direction.



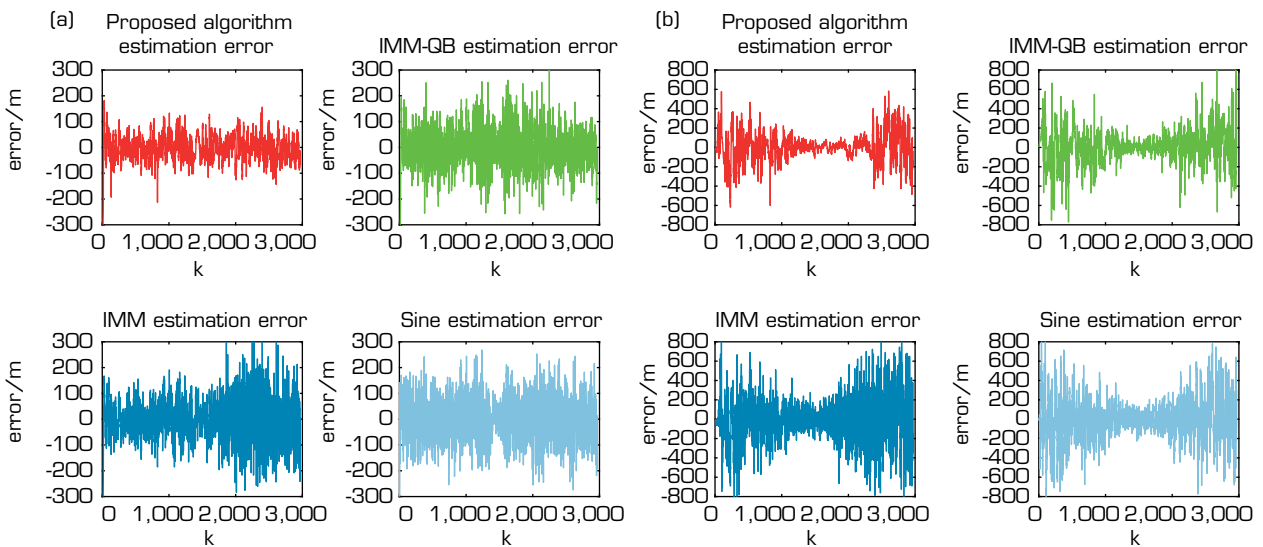
Simulation result

The tracking results of the HGV trajectory 1 employing the four methods are depicted in Fig. 5. Figure 6a and b show the estimation error of the four tracking algorithms. Figure 6 illustrates that during the process of filtering and tracking the target state in formation, the trajectory produced by the adaptive variable structure IMM algorithm closely aligns with the actual trajectory. The simulation results indicate that, in comparison with both the IMM-QB algorithm and the classical IMM algorithm, the proposed algorithm has demonstrated favorable outcomes and greater stability in target tracking. During the target tracking process, if the RMSE surpasses a predefined threshold during single-model tracking, the proposed algorithm dynamically switches to the multi-model tracking approach at the current time to re-track the maneuvering target. Consequently, in contrast to the other two multi-model tracking methods, the proposed algorithm exhibits minimal error fluctuations.



Source: Elaborated by the authors.

Figure 5. Comparison rendering of the real trajectory 1 of the target and the tracking trajectory of the target using the four methods.



Source: Elaborated by the authors.

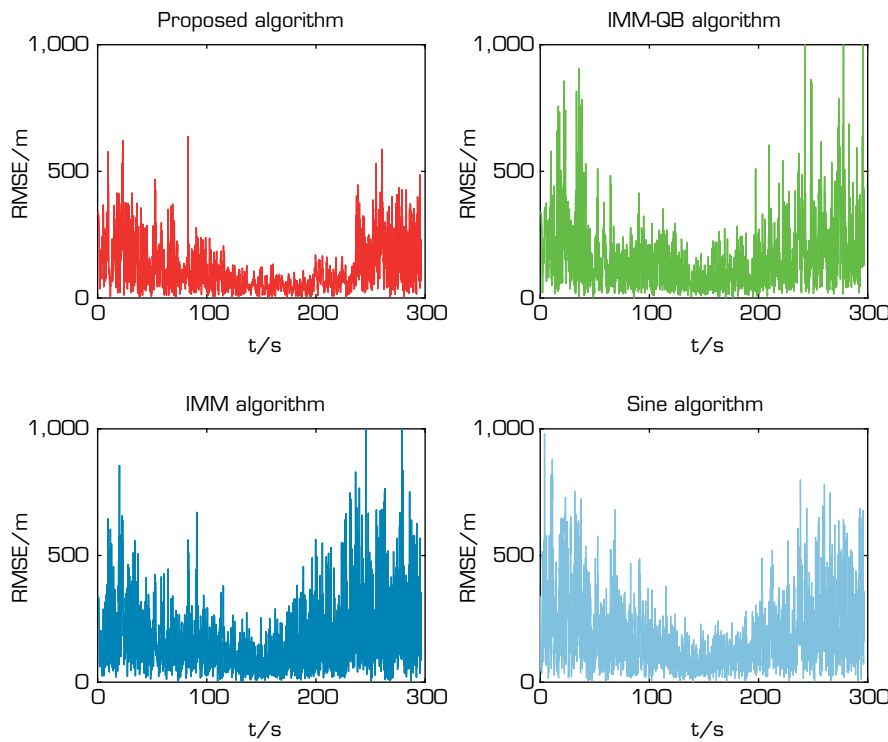
Figure 6. Position estimation errors for the four algorithms in the trajectory 1 X and Y directions. (a) X direction; (b) Y direction.

A Monte Carlo mathematical simulation is conducted for the maneuvering target tracking model, with the RMSE of position serving as the performance metric. The position RMSE at time k is defined as follows:

$$RMSE_p(k) = \sqrt{\frac{1}{N} \sum_{n=1}^N ((x_k^n - \hat{x}_k^n)^2 + (y_k^n - \hat{y}_k^n)^2)} \quad (12)$$

where N represents the number of Monte Carlo iterations and (x_k^n, y_k^n) and $(\hat{x}_k^n, \hat{y}_k^n)$ denote the true value and the estimated value of the target position at the time k of the n iteration, respectively.

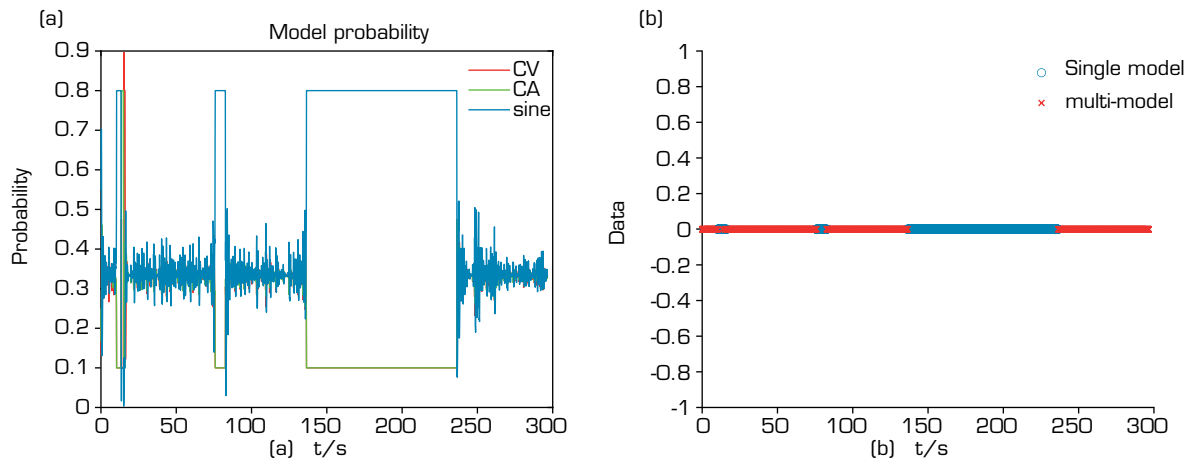
Upon examining the position RMSE of the four algorithms in Fig. 7, it is evident that the proposed algorithm may exhibit occasional spikes in position RMSE at certain instances. However, its performance demonstrates relative stability in general. Figure 8a and b indicate that the sine model is used several times during the tracking process using the proposed adaptive variable structure IMM algorithm. The local maneuvering pattern exhibited by the target closely resembles that of the sine model. However, relying solely on the sine model is insufficient to comprehensively describe the entirety of the target's maneuvering pattern. Hence, the adaptive variable structure IMM tracking algorithm enhances tracking accuracy by dynamically switching between single and multiple models based on the prevailing circumstances. The RMSE values and running times of the four algorithms for the four trajectories tracking are shown in Table 3.



Source: Elaborated by the authors.

Figure 7. The position RMSE of the four algorithms for trajectory 1.

Compared with the simulation results of several tracking algorithms, the proposed algorithm adopts a single/multi-model adaptive transformation method to obtain the minimum RMSE value. The single-model tracking algorithm has the shortest running time, and the IMM-QB algorithm has the longest running time. In contrast, the IMM-QB algorithm is superior to the IMM in tracking accuracy, but its running time is longer. Although the sine algorithm has the shortest running time, the corresponding RMSE is significantly higher than that of the other algorithms. In short, this algorithm can guarantee the tracking accuracy while maintaining a small running time, which is its most comprehensive advantage.



Source: Elaborated by the authors.

Figure 8. Distribution diagram of trajectory 1 tracked by the adaptive variable structure IMM algorithm. (a) Model probability; (b) Single-multiple model.

Table 3. Performance comparison table of several tracking algorithms.

Method	RMSE (m)				Running time (s)			
	1	2	3	4	1	2	3	4
AVSIMM	150.62	206.62	129.41	162.45	0.986	1.046	0.829	0.975
IMM-QB	200.50	231.84	218.52	194.67	1.340	1.313	1.217	1.355
IMM	216.56	247.78	246.39	226.83	1.273	1.292	1.188	1.264
Sine	236.18	295.29	270.36	246.78	0.379	0.377	0.378	0.375

Source: Elaborated by the authors.

Although the sine algorithm has obvious advantages in running time, its insufficient tracking accuracy limits its application range. The interactive multiple model algorithm based on the quasi-Bayesian (IMM-QB) algorithm and the IMM algorithm perform well in application scenarios requiring high tracking accuracy, but the long running time affects real-time performance. Therefore, the proposed algorithm achieves a balance between tracking accuracy and running time, making it most suitable for application environments that require both high efficiency and tracking accuracy. In general, hypersonic maneuvering targets have strong maneuvering ability but low maneuvering frequency. Relying solely on multi-model tracking may lead to less efficient operations. Therefore, the single/multiple model variable structure tracking algorithm proposed in this paper aims to improve the tracking accuracy, stability, and operational efficiency.

CONCLUSION

Given the challenges posed by model stability matching and the computational complexity inherent in maneuvering target tracking algorithms, this paper introduces an adaptive variable structure tracking algorithm integrated with the unscented Kalman filter algorithm. Compared with existing methods, the proposed method cannot achieve real-time tracking of hypersonic maneuvering targets in near space, but also adaptively select the tracking model (single model or multiple models) according to the motion pattern of the target. It effectively solves the problems of unstable matching in single model algorithms and the computational redundancy of traditional multi-model tracking algorithms. Additionally, it incorporates two correction functions into the IMM algorithm to dynamically update the probability transition matrix. Simulation results show that the proposed method can reduce single computation time by nearly one-fourth times while maintaining the tracking accuracy. The model set employed

in this study comprises three mathematical models. As the duration of target motion increases and the model set expands, the effectiveness of the proposed method becomes more pronounced.

CONFLICT OF INTEREST

Nothing to declare.

AUTHORS' CONTRIBUTION

Conceptualization: Fu Z, Wan D, Wang Z, and Tao F; **Methodology:** Fu Z, Wan D, Wang Z, and Tao F; **Validation:** Fu Z, Wan D, and Wang Z; **Writing - Original Draft:** Fu Z, Wan D, and Wang Z; **Writing - Review & Editing:** Wan D, Wang Z, and Tao F; **Final approval:** Wang Z.

DATA AVAILABILITY STATEMENT

Data sharing is not applicable.

FUNDING

Joint funding from National Key Laboratory of Air-based Information Perception and Fusion and the Aeronautical Science Foundation of China

Grant No: 20220001042002

Henan Province Key Scientific and Technological Projects

Grant No: 242102221025

Key Scientific Research Projects of Universities in Henan Province

Grant No: 24B590001

ACKNOWLEDGEMENTS

Not applicable.

REFERENCES

Biao Y, Sheng Z, Kun Y (2021) Multi-sensor multiple maneuvering targets tracking algorithm under greedy measurement partitioning mechanism. *Journal of Electronics and Information Technology* 43(7):1962-1969. <https://doi.org/10.11999/JEIT200498>

Cheng YP, Yan XD, Tang S (2021) An adaptive non-zero mean damping model for trajectory tracking of hypersonic glide vehicles. *Aerosp Sci Technol* 111:106529. <https://doi.org/10.1016/j.ast.2021.106529>



- Feng Y, Wang H, Qu ZG, Li F, Dong YH (2020) Hypersonic gliding target tracking based on improved jerk model. *Journal OF Air Force Engineering University (Natural Science Edition)* 21(1):80-86. <https://doi.org/10.3969/j.issn.1009-3516.2020.01.013>
- Garcia-Fernandez ÁF, Morelande MR, Grajal J (2012) Truncated unscented Kalman filtering. *IEEE Trans Signal Process* 60:3372-3386. <https://doi.org/10.1109/tsp.2012.2193393>
- Guo Q, Teng L (2022) Maneuvering target tracking with multi-model based on the adaptive structure. *IEEJ Trans Electr Electron Eng* 17(6):865-871. <https://doi.org/10.1002/tee.23575>
- Jia SY, Zhang Y, Wang GH (2017) Highly maneuvering target tracking using multi-parameter fusion singer model. *Syst Eng Electron* 28(5):841-850. <https://doi.org/10.21629/jsee.2017.05.03>
- Jiang K, Zhou JJ (2022) A single maneuvering target tracking algorithm based on STUKF for automotive radar. Paper presented 2022 International Conference on Signal Processing and Communication Technolog. Xidian University; Harbin, China. <https://doi.org/10.1117/12.2631820>
- Jilkov VP, Li XR (2004) Online Bayesian estimation of transition probabilities for Markovian jump systems. *IEEE Trans Signal Process* 52(6):1620-1630. <https://doi.org/10.1109/tsp.2004.827145>
- Jordi VV, Damien V (2020) Recursive linearly constrained Wiener filter for robust multi-channel signal processing. *Signal Process* 167:107291. <https://doi.org/10.1016/j.sigpro.2019.107291>
- Lee IH, Park CG (2023) An improved interacting multiple model algorithm with adaptive transition probability matrix based on the situation. *Int J Control Autom Syst* 21(10):3299-3312. <https://doi.org/10.1007/s12555-022-0989-4>
- Li F, Xiong JJ, Chen X, Qu ZG, Bi HK, Zhang JB, Xi QS (2022) Near space hypersonic vehicle target tracking adaptive non-zero mean model. *IEEE Access* 10:30445-30456. <https://doi.org/10.1109/access.2021.3139434>
- Li F, Xiong JJ, Qu ZG, Lan XH (2020) A damped oscillation model for tracking near space hypersonic gliding targets *IEEE Trans Aerosp Electron Syst* 55(6):2871-2890. <https://doi.org/10.1109/taes.2019.2897517>
- Li L.Q, Zhan XY, Xie WX, Liu ZX (2021) Interacting T-S fuzzy semantic model estimation for maneuvering target tracking. *Neurocomputing* 421:84-96. <https://doi.org/10.1016/j.neucom.2020.08.067>
- Li LQ, Xie WX, Liu ZX (2016) Auxiliary truncated particle filtering with least-square method for bearings-only maneuvering target tracking. *IEEE Trans Aerosp Electron Syst* 52(5):2564-2569. <https://doi.org/10.1109/taes.2016.150048>
- Luo Y, Li Z, Liao Y (2022) Adaptive Markov IMM based multiple fading factors strong tracking CKF for maneuvering hypersonic-target tracking. *Appl Sci* 12(20):10395. <https://doi.org/10.3390/app122010395>
- Montañez OJ, Suarez MJ, Fernandez EA (2023) Application of data sensor fusion using extended Kalman filter algorithm for identification and tracking of moving targets from LiDAR-radar data. *Remote Sens* 15:3396. <https://doi.org/10.3390/rs15133396>
- Song L, Li X, Liu Y (2021) Effect of time-varying plasma sheath on hypersonic vehicle-borne radar target detection. *IEEE Sens J* 21(15):16880-16893. <https://doi.org/10.1109/jsen.2021.3077727>
- Sun W, Yang Y (2016) Adaptive maneuvering frequency method of current statistical model. *IEEE/CAA J Automatic* 4(1):154-160. <https://doi.org/10.1109/jas.2016.7510130>
- Wang GH, Li JJ, Zhang XY (2015) A tracking model for near space hypersonic slippage leap maneuvering target. *Acta Aeronaut Astronaut Sin* 36(7):2400-2410. <https://doi.org/10.7527/S1000-6893.2014.0160>



- Wang X, Xu Z, Gou X, Trajkovic L (2020) Tracking a maneuvering target by multiple sensors using extended Kalman filter with nested probabilistic-numerical linguistic information. *IEEE Trans. Fuzzy Syst* 28(2):346-360. <https://doi.org/10.1109/TFUZZ.2019.2906577>
- Xie G, Sun L, Wen T, Hei X, Qian F (2019) Adaptive transition probability matrix-based parallel IMM algorithm. *IEEE Trans Syst Man Cybern A:Syst* 51(5):2980-2989. <https://doi.org/10.1109/tsmc.2019.2922305>
- Xu X, Yan X, Yang W, Kay A, Huang W, Wang Y (2022) Algorithms and applications of intelligent swarm cooperative control: a comprehensive survey. *Prog Aersp Sci* 135:100869. <https://doi.org/10.1016/j.paerosci.2022.100869>
- Ye J, Xu F, Yang J (2020) An improved AIMM tracking algorithm based on adaptive transition probability. *Appl Acoust* 39(2):246-252. <https://doi.org/10.11684/j.issn.1000-310X.2020.02.011>
- Yu CL, Tan XS, Qu ZG, Wang H, Xie F (2019) Marginal tracking algorithm for hypersonic reentry gliding vehicle. *IET Radar Sonar Nav* 13(1):156-166. <https://doi.org/10.1049/iet-rsn.2018.5192>
- Yu W, Chen W (2021) High-accuracy approximate solutions for hypersonic gliding trajectory with large lateral maneuvering range. *IEEE Trans Aerosp Electron* 57(3): 1498-1512. <https://doi.org/10.1109/taes.2020.3043532>
- Zhang J, Xiong J, Lan X, Shen Y, Chen X, Xi Q (2022) Trajectory prediction of hypersonic glide vehicle based on empirical wavelet transform and attention convolutional long short-term memory network. *IEEE Sens J* 22(5):4601-4615. <https://doi.org/10.1109/jsen.2022.3143705>
- Zhao CC, Wang Z, Ding G (2021) Fuzzy-logic adaptive IMM algorithm for target tracking. *J Signal Process Syst* 37(5):724-734. <https://doi.org/10.16798/j.issn.1003-0530.2021.05.005>